p53 isoform Δ113p53/Δ133p53 promotes DNA double-strand break repair to protect cell from death and senescence in response to DNA damage

1

of environmental factors, such as ionizing radiation and various chemical agents (e.g., methyl methanesulfonate and bleomycin), can cause DNA DSBs
such DNA damage stress conditions, it is very important for an organism to decide which cells are non-repairable and thus can be induced to die and which cells are re pairable and thus can survive after DNA damage repair. However, how these decisions are made in response to DNA DSBs remains unexplored.

A central part of the DNA damage response is the activation of the tumor repressor gene, *p53*. Upon acti vation, p53 upregulates or represses the expression of a large number of downstream genes. The promoters of genes activated by p53 usually contain a consensus se quence of two pairs (half-sites) of pentamers arranged head-to-head, 5′-RRRC(A/T)(A/T)GYYY-3′ (R: pu rine, Y: pyrimidine), separated by 0-38 nucleotides. The promoters of genes repressed by p53 usually contain a consensus sequence of two pairs of pentamers arranged end-to-head, 5′-RRRC(A/T)(N)RRRC(A/T)-3′ ′-(A/ T)GYYY(N)(A/T)GYYY-3′ (N: purine or pyrimidine), separated by 0-13 nucleotides . The expression of p53 downstream genes triggers cell cycle arrest, DNA damage repair, apoptosis and/or senescence to ensure ge nome stability . Intriguingly, p53 protein appears to promote only some DNA damage repair pathways, such as base excision repair, mismatch repair and nucleotide excision repair , but inhibit DNA DSB repair path ways, including the HR, NHEJ and SSA pathways . It has been demonstrated that p53 exerts a direct ef fect on DNA DSB repair, as mutations in p53 that impair or even abolish its transcriptional activity and cell cycle regulatory capacity do not signi fcantly affect its inhibi tion of HR . Further experiments have shown that the p53 protein is able to interact with repair proteins to prevent repair complex formation, such as RAD51 (a recombinase for HR) and replication protein A (RPA; a single-strand DNA-interacting protein required for sta bilizing processed DNA ends) . In contrast, there is also evidence that p53 transcriptionally inhibits the expression of repair genes, such as *RAD51* . Re cent studies have shown that the p53 protein relies on dynamic changes in its levels to control cell fate in re sponse to DNA DSB stress, such as γ-irradiation, which is quite different from a single p53 pulse induced by UV irradiation . Therefore, although full-length p53 inhibits DNA DSB repair, it is not clear how the p53 signal pathway regulates DNA DSB repair in response to DNA DSB stress.

The zebrafish protein Δ113p53 and its human coun terpart Δ133p53 are N-terminally truncated forms of p53 with deletion of both the MDM2-interacting motif and the transactivation domain, together with partial deletion of the DNA-binding domain . Δ*113p53/*Δ*133p53* is a p53 target gene, which is transcribed by an alterna tive *p53* promoter in intron 4. It is strongly induced by DNA damage stress to antagonize p53-mediated apopto . Our previous studies showed that Δ113p53 does not act on p53 in a dominant-negative manner, but rather interferes with p53 function by differentially mod ulating p53 target gene expression to protect cells from apoptosis . Δ133p53 also represses cell replication senescence and promotes angiogenesis and tumor . However, knowledge of its function in DNA DSB repair is lacking.

In this study, we demonstrate that Δ113p53/Δ133p53 is strongly accumulated at the later stage in response to DNA DSB signals, such as γ-irradiation, to promote all three DNA DSB repair pathways in both zebra fsh and human cells. We also demonstrate that Δ113p53/Δ133p53 regulates DNA DSB repair by transcriptionally upreg ulating the expression of *RAD51 LIG4 RAD52* independent of full-length p53. Our fndings provide an important clue to unravel the perplex of p53 in the DSB

Results

treatment

We showed previously that expression is induced by γ-irradiation . In the current study, we ex amined the expression of in zebra fsh embryos after UV irradiation and heat shock treatment. We found that although upregulation of full-length p53 expression reached a similar level upon different treatments, the expression of was only induced by 16 gray of γ-irradiation and was not, or only weakly, induced by other treatments (Figure 1A and Supplementary informa tion, Figure S1A). This induction appears to be a speci fc outcome of γ-irradiation treatment, because there was no, or only a low-level, induction of expres sion even when embryos were exposed to harsher UV or higher temperature conditions that caused most em bryos to die at 32 hours post treatment (hpt). In contrast, almost 100% of embryos treated with 16 gray of γ-irra diation survived at 32 hpt (Supplementary information, Figure S1B). Upon exposure to γ-irradiation, p53 levels peaked as early as 4 hours post irradiation (hpi), where as Δ113p53 levels peaked later, at 24 hpi (Figure 1B As the main difference in the damage induced by the different treatments was that only γ-irradiation led to ge nome-wide DNA DSBs, we speculated whether the high

Figure 1 Zebrafsh Δ113p53 promotes DSB repair. **(A)** Western blot of zebrafsh p53 and Δ113p53 from the untreated control (untreated) and embryos treated with γ-ray, UV irradiation (UV) or heat shock (HS) at 8 hpt using the A7-C10 monoclonal antibody against zebrafsh p53. β-tubulin was used as the protein loading control. **(B)** Kinetics of p53 and Δ113p53 protein expression in zebrafsh embryos treated with 16 gray of γ-ray irradiation or untreated. Total protein stained with Coomassie blue was used as the loading control. h: hours after treatments. **(C)** Effects of zebrafsh p53 and Δ113p53 on HR, NHEJ and SSA repair frequencies. The average repair frequencies were measured using a qPCR analysis of the repair assay constructs (Supplementary information, Figure S2) from three repeat experiments at 10 hpf. Different lanes are numbered; v: versus, *t*-test between two lanes. **(D)** Western blot of p53 and Δ113p53 in different embryos as indicated. Proteins were extracted from non-irradiated and irradiated embryos at 8 hpi. **(E)** Assessment of DNA DSB with a comet assay in different embryos as indicated. Individual cells were dissociated at 28 and 36 hpi and used in the comet assay. 130-900 cells from each sample

level of Δ113p53 induced by γ-irradiation might play a role in DNA DSB repair.

To test our hypothesis, we used three Egfp-repair ing-aided visual-plus-quantitative analysis reporter sys tems to measure HR, NHEJ and SSA repairs plementary information, Figure S2). The corresponding plasmids were linearized with I-*Sce*I, and then co-in jected with *p53* morpholino (p53-MO, which targets the ATG of full-length *p53* mRNA to block its translation), morpholino (Δ113p53-MO, which speci f cally targets the 5′-UTR of mRNA) MO-plus- mRNA mix into zebra f sh wild-type (WT) embryos. The linearized plasmid DNA was also co-injected into *p53*^{M214K} mutant embryos (*p53*^{M214K} carries an M214-to-K214 substitution in the DNA-binding do) with *p53* mRNA, mRNA or a *p53* plus- mRNA mix (Supplementary information, Figure S3). Protein analysis showed that injection of lin earized plasmid alone activated the p53 pathway, which further induced expression in WT embryos (Supplementary information, Figure S4). We con f rmed DSB repair in each treatment at 8 hours post fertilization (hpf), by either EGFP fluorescence intensity measure ment or quantitative real-time PCR (qPCR) analysis of the repaired *Egfp* DNA fragments. Our results showed that zebrafish p53, like human p53, inhibited all three DNA DSB repair pathways at 8 hpf (, lanes 3 vs 1 and 7 vs 5, and Supplementary information, Figure S5). Knockdown of Δ113p53 signi f cantly enhanced the inhibitory effect of the endogenous p53 on DSB repair , lanes 2 vs 1, and Supplementary information, Figure S5). In contrast, the overexpression of Δ113p53 promoted all three DSB repair pathways in *p53* mutant , lanes 6 vs 5, and Supplementary information, Figure S5). To investigate whether p53^{M214K} and Δ113p53^{M214K} mutant proteins have a gain-of-func tion effect on DNA DSB repairs, we co-injected the lin earized repair plasmids with either p53-MO or Δ113p53-MO into *p53*^{M214K} mutant embryos (Supplementary infor mation, Figure S6). The qPCR analysis of the repaired *Egfp* DNA fragments showed that knockdown of either ^{M214K} or Δ113p53^{M214K} mutant protein had little effects on HR, NHEJ and SSA repairs, suggesting that both mutant proteins do not have a gain-of-function effect on DNA DSB repairs.

We next investigated the influence of Δ113p53 on DNA DSB repair of genomic DNA using a comet assay (single cell gel electrophoresis) by analyzing the genom ic DNA damage induced by γ-irradiation in zebrafish embryos (Supplementary information, Figure S7). WT *p53*^{M214K} mutant embryos were injected with either the standard control morpholino (Std-MO, against hu man β-globin) or Δ113p53-MO. The injected WT and *p53*^{M214K} mutant embryos were treated with 16 gray of γ-irradiation ( ). A TUNEL assay showed that apoptosis decreased to the basal level after 24 hpi (Sup plementary information, Figure S8). We thus used 28-hpi and 36-hpi irradiated embryos to detect the levels of DNA DSB, minimizing the interference of apoptosis in the assay. Our results showed that the extent of DNA damage in WT embryos with Δ113p53 knockdown was ~2-fold of that in the irradiated control embryos at either Figure 1E). Very interestingly, the ex tent of DNA damage dropped faster in WT embryos (from 4.76 at 28 hpi to 0.37 at 36 hpi, 12.86-fold) than in the *p53*^{M214K} mutants (from 2.72 at 28 hpi to 0.59 at 36 hpi, ~4.6-fold), which correlated well with the presence of Δ113p53 accumulation in WT and its absence in *p53*^{M214K} embryos induced by γ-irradiation (Figure 1D and 1E Notably, the extent of DNA damage in the irradiated WT embryos (4.76) was signi f cantly higher than that in the irradiated *p53*^{M214K} embryos (2.72) at 28 hpi. In contrast, at 36 hpi, the extent of DNA damage was signi f cantly lower in the irradiated WT (0.37) than in the irradiated *p53*^{M214K} embryos (0.59). One possible explanation for this observation is that full-length p53 is induced to a high level at the early stage (Figure 1B) in WT embryos after irradiation, which could guide the cells with severe DNA damage towards apoptosis while repressing DNA DSB repair in the surviving cells. On the other hand, due to the lack of bioactive p53, the DNA-damaged cells in the *p53*^{M214K} mutant were still able to undergo the DNA DSB repair. Hence, we observed that the extent of DNA damage was higher in WT than that in *p53*^{M214K} at 28 hpi. At 36 hpi, the expression of Δ113p53 in WT embryos ac cumulated to a high level, which in turn blocked apopto sis and promoted DNA DSB repair in the surviving cells. This resulted in a drastic drop in the extent of DNA dam age in these WT cells. However, in the irradiated *p53*^{M214K} embryos, although the DNA-damaged cells were able to undergo DNA DSB repair, the repair ef f ciency was low due to the absence of expression (Furthermore, the irradiated *p53*^{M214K} embryos contained a large number of non-repairable cells with severe DNA damage, which escaped apoptosis in the absence of the bioactive p53. As a result, cells in *p53*^{M214K} embryos ex hibited signi f cantly higher levels of DNA damage than those in WT embryos at 36 hpi. These results demon strate the importance of the coordination of p53 and Δ113p53 functions at the organismal level to minimize DNA damage upon DNA DSB stress.

M/M mutant

To study the biological significance of Δ113p53 in DNA DSB repair, we generated a zebrafish Mutation/mutation M/M knockout mutant. As the coding sequence is completely overlapped with the full-length *p53*, we chose to knock out by targeting its promoter. One of our previous studies showed that the promoter is located in the fourth intron of the full-length *p53* gene and contains three putative p53 response elements (REs) Figure 2A) . A subsequent study showed that the third p53 RE is required for expression (unpublished data). Therefore, we generated a mutant by targeting the third p53 RE in its promoter with the transcription activator-like effector nuclease (TALEN) technique. One mutant was obtained with an 11-bp deletion, which includes an 8-bp sequence within the third p53 RE (Figure 2A). Western blot showed that the induction of expression was almost completely blocked, whereas the activation of full-length p53 was unaffected in the M/M tants in response to γ-irradiation (Figure 2B

M/M -

radiation due to loss of functions in anti-apoptosis and promoting DNA DSB repair

M/M mutant fsh grows to adulthood normally in standard growth conditions. To test whether three DNA DSB repair pathways are affected in the mutant, the I-*Sce*I-linearized HR, NHEJ or SSA plasmid was injected into WT and M/M embryos, and was co-injected with mRNA into M/M embryos. Results showed that the efficiency of the three DNA DSB repair pathways was significantly decreased in M/M embryos (Supplementary information, Figure S9), which is similar to that observed in the Δ113p53-MO-injected). The efficiency of all three repair pathways was restored by mRNA co-injection (Supplementary information, Figure S9), demonstrating that the decrease of DNA DSB repair efficiency in M/M embryos was due to the absence of

We then treated WT and M/M embryos with γ-irradiation. Assessment of embryo viability revealed that the M/M embryos (all of which died at 5 dpi) were much more susceptible to γ-irradiation than WT embryos (~30% of which was viable at 5 dpi;). Two main functions of Δ113p53 have been demonstrated, i.e., to antagonize the pro-apoptotic function of p53 and to promote DNA DSB repair. To determine the contribution of Δ113p53's DSB repair function to the high mortality rate in the mutant embryos in response to γ-irradiation, we blocked cell apoptosis by injecting *bcl2L* (anti-apoptotic protein) mRNA into WT and M/M embryos. Western blot showed that *bcl2L* mRNA injection did not influence the induction of Δ113p53 (Figure 2B). Similar to the results in embryos injected with 113p53-MO , more apoptotic cells were observed in M/M embryos than in WT embryos upon γ-irradiation (Figure 2E). However, irradiation-induced apoptosis was almost completely inhibited *bcl2L* mRNA injection in both WT and M/M Figure 2E). The viability of irradiated mutant embryos injected with *bcl2L* mRNA (~20% at 5 dpi) was significantly lower than that of WT embryos (~50%) with the same treatment, and even lower than that of irradiated WT embryos (~30%) without *bcl2L* mRNA injection (albeit with abundant apoptotic cells;

Comet assay results showed that *bcl2L* mRNA injection slightly increased the extent of DNA damage in both irradiated WT and M/M embryos at a similar scale. This increase occurred possibly because Bcl2L overexpression prevented cells with severe DNA damage from apoptosis in both irradiated WT and M/M). Conversely, mRNA injection restored the viability of irradiated mutant embryos to the WT level upon γ-irradiation (Supplementary information, Figure S10). Taken together, these results suggest that loss of both functions of Δ113p53 (i.e., anti-apoptosis and promotion of DNA DSB repair) renders M/M embryos more sensitive to γ-irradiation.

The promotion of DNA DSB repair is conserved in hu-

We treated human QSG-7701 cells (a non-cancerous liver epithelial cell line containing WT *p53*) with γ-irradiation, UV irradiation and heat shock, and analyzed the function of the human ortholog, Δ133p53, in DNA DSB repair. Both Δ133p53 transcript and protein were strongly induced by γ-irradiation only (Figure 3A; Supplementary information, Figure S11A-S11C). We then transfected the H1299 cells (which lack the endogenous *p53* with each of the three visual-plus-quantitative assay constructs, along with *p53* *p53*-plus- mRNA (Supplementary information, Figure S12). Both qPCR analysis of the repaired *Egfp* DNA fragments and fluorescence-activated cell sorting (FACS) analysis of EGFP-positive cells revealed that, apart from neutralizing the DSB repair inhibitory effect of full-length p53, Δ133p53 also almost doubled the efficiency of all the three DNA DSB repair pathways in a p53-independent manner, compared to their corresponding controls (ure 3B and Supplementary information, Figure S13). To study the function of endogenous Δ133p53 in DNA DSB repair, we co-transfected each of the three repair assay constructs with either a non-specific siRNA control

Figure 2 Zebrafish Δ*113p53*$^{M/M}$ mutant is more sensitive to γ-irradiation. **(A)** Diagram showing the Δ*113p53* promoter and an 11-bp deletion in the promoter of Δ*113p53*$^{M/M}$ mutant. TSS: transcription start site of Δ*113p53*. RE: p53 response element. The numbers indicate the positions in the Δ*113p53* promoter. Out of the deleted 11 bp, 8 bp are within the RE3. **(B)** Western blot analysis of p53 activation and Δ113p53 induction in WT and Δ*113p53*$^{M/M}$ embryos injected or uninjected with *bcl2L* mRNA, followed by 16 gray of γ-ray irradiation. **(C**, **D)** WT and Δ*113p53*$^{M/M}$ embryos with or without injection of *bcl2L* mRNA at 1 dpf were treated with γ-irradiation. The pictures were taken at 5 dpi **(C)**. The average viabilities of embryos with different treatments were taken from three repeats from 1 to 7 dpi as indicated **(D)**. **(E)** A TUNEL assay was used to examine apoptotic cells in embryos with different treatments at 8 hpi as indicated. Approximately 20 embryos from each treatment were sampled at each time point. **(F)** Assessment of DNA DSB by a comet assay in embryos with different treatments as indicated at 2 dpi.

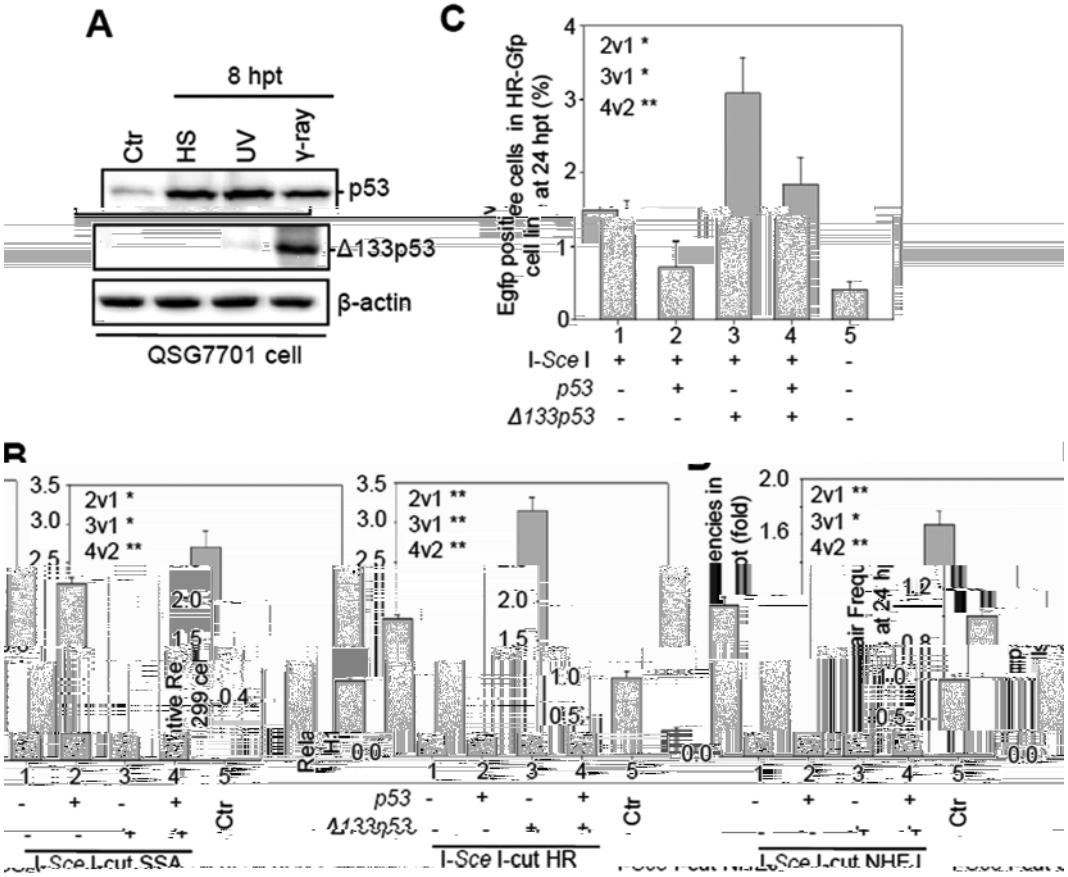

Figure 3 Human Δ133p53 promotes HR, NHEJ and SSA repair pathways. **(A)** Western blot of human p53 and Δ133p53 from human QSG7701 cells treated as indicated using a monoclonal antibody DO-1 and a polyclonal antibody CM1, respectively. β-actin was used as the protein loading control. **(B)** Effect of human Δ133p53 on HR, NHEJ and SSA repair frequencies. Relative DNA DSB repair frequencies for HR, NHEJ and SSA were measured by qPCR at 24 hpt. **(C)** Effect of Δ133p53 on HR repair frequency in the U2OS (HR-GFP) cell line. *CMV-I-Sce*I plasmid was transfected or co-transfected with *CMV-p53*, *CMV-Δ133p53* or *CMV-p53*-plus-*CMV-Δ133p53*

(siNS) or two siRNAs, siRNA1 (Δ133p53i-1) or siRNA2 (Δ133p53i-2; both targeting 5′-UTR of located in the intron 4 of full-length *p53* into QSG-7701 cells (Supplementary information, Figure S14A). The qPCR analysis showed that the knockdown of Δ133p53 significantly decreased the efficiencies of the three DNA DSB repair pathways (Supplementary information, Figure S14B). The positive role of Δ133p53 in DNA DSB repair was also observed in U2OS cells ( ), which harbor WT p53 and stably express HR-GFP

It has been reported that human p53 inhibits RAD51 foci formation in response to DNA damage . We used QSG-7701 cells to study the function of Δ133p53 in the formation of the DNA DSB repair foci of phosphorylated H2AX (γH2AX; which is one of the early DNA DSB repair markers) and RAD51 upon -irradiation. QSG-7701 cells were transfected with either a non-specific siRNA control (siNS), a *p53* siRNA (p53i; targeting exon 4 of full-length p53) , or two siRNAs, Δ133p53i-1 and Δ133p53i-2, and treated with 10 gray of -irradiation (Figure 4A). Our results confirmed that p53 has a negative influence on RAD51 foci formation (ure 4B and 4C; Supplementary information, Figure S15). In contrast, overexpression of Δ133p53 significantly increased RAD51 foci formation at 12 hpi upon γ-irradiation, whereas knockdown of endogenous Δ133p53 significantly decreased foci formation under the same conditions (Figure 4B, 4C and Supplementary information, Figure S15). Our results also showed that the formation of γH2AX foci was not significantly affected by Δ133p53 or p53 overexpression, suggesting that Δ133p53 and p53

may not have a significant effect on the early steps of DNA DSB repair (Figure 4B, 4C Supplementary in formation, Figure S15).

FACS analysis revealed, as expected, that the number of apoptotic cells (sub-G0 summit) was decreased by p53 knockdown from 8 to 24 hpi and was increased by Δ133p53 knockdown from 4 to 24 hpi (Supplementary information, Figure S16) . However, apoptosis decreased to the basal level by 36 hpi in all cases (Sup plementary information, Figure S16). Therefore, we performed the comet assay at 48 hpi to test whether the decrease in the number of RAD51 foci upon Δ133p53 knockdown was accompanied by an increase in DNA damage. Comet assay results showed ~1.5-fold greater damage in cells transfected with the Δ133p53 siRNAs than in the irradiated control cells (results demonstrate that Δ133p53 plays a positive role in genomic DNA DSB repair upon γ-irradiation. However, the extent of DNA damage in irradiated control cells (1.0) was only slightly lower than that in irradiated p53-knock down cells (1.1) at 48 hpi ( ), which differed from the comet assay results obtained from irradiated zebrafish WT and *p53*^{M214K} embryos at 36 hpi (1E). One likely explanation is that in embryos, apoptotic cells are cleared away by other cells *in vivo*, while in cell culture conditions, there is no such system to remove the apoptotic cells, which may interfere with the comet assay carried out in cultured cells.

-

liferation through arresting cell cycle at the G2 phase

To study the consequence of increased DNA damage at the cellular level, we transfected QSG-7701 cells with siNS, Δ133p53i-1, or 133p53i-2 and treated them with 10 gray of γ-irradiation. As described above, apoptosis decreased to the basal level at 36 hpi (Supplementary information, Figure S14). We washed away apoptotic cells at 2 dpi and replaced with a new culture medium to allow the remaining cells to grow under normal condi tions. At 5 dpi, total cell number and colony size (which showed flattened cell morphology) were observably decreased by the treatment of γ-irradiation, compared to those of unirradiated controls (Figure 5A). Interestingly, after γ-irradiation fewer cell numbers and a smaller colo ny size were observed in cells transfected with Δ133p53 siRNA compared with the siNS-transfected control Figure 5A), which correlates well with the extent of DNA damage observed ( ). FACS analysis of cells at 5 dpi showed that the proportion of cells at the G2 phase increased slightly, from 14.1% to 19.6%, in siNS-transfected cells, but almost doubled from 16.8% to 35.5% in Δ133p53i-1- and from 17.6% to 34.6% in Δ133p53i-2-transfected cells (Figure 5B). In contrast, there was little difference in the proportion of cells at the S phase between the irradiated cells and untreated con trols (Figure 5B). These results suggest that a high level of DNA damage results in cell cycle arrest at the G2

Next, cell senescence analysis was performed with senescence-associated β-galactosidase (SA-β-gal) staining. The occurrence of positive cells (about 89% in Δ133p53i-1- and 80% in Δ133p53i-2-transfected cells) at 5 dpi was significantly increased by Δ133p53 knockdown upon γ-irradiation, compared to that in the irradiated siNS control (about 40%; Supplementary information, Figure S17). Taken together, loss of function of Δ133p53 increased DNA DSBs upon γ-irradiation, which in turn inhibited cell proliferation by arresting cell cycle at the G2 phase, finally resulting in cell senescence.

RPA

It was proposed that the p53 protein directly interacts with either RAD51 or RPA to inhibit DNA DSB repair complex formation. Previous studies have shown that the DNA-binding core domain (94-312) of p53 is required for p53-RAD51 interactions, and its N-terminal domain (37-57) is required for p53-RPA in teractions , which suggests that Δ133p53 may not be able to form a complex with these two proteins. We performed a co-immunoprecipitation (co-IP) experiment to test this hypothesis by co-transfecting HA-RAD51 or HA-RPA2 with p53, Δ133p53 or both, into H1299 cells. The results showed that full-length p53 (Figure 6A, lanes 2 and 10), but not Δ133p53 (Figure 6A, lanes 3 and 11) formed a complex with either HA-RAD51 or HA-RPA2. It was observed that the protein level of RAD51, RPA2 or Δ133p53 was dramatically decreased when it was co-expressed with full-length p53 in the experiments, but the reason is currently not known.

DNA DSB repair genes

We investigated the molecular mechanisms by which Δ113p53/Δ133p53 promotes DNA DSB repair inde pendent of p53. We co-injected a linearized plasmid (to mimic DNA DSB stress) with either *p53* *p53*-plus- mRNA into *p53*^{M214K} mutant embryos and analyzed the expression of DSB- and p53-response genes by quantitative reverse transcription PCR (qRT-PCR). Unlike two p53-responsive genes, *p21* (a cell cycle inhibitor) and *mdm2* (an E3 ligase), the expression

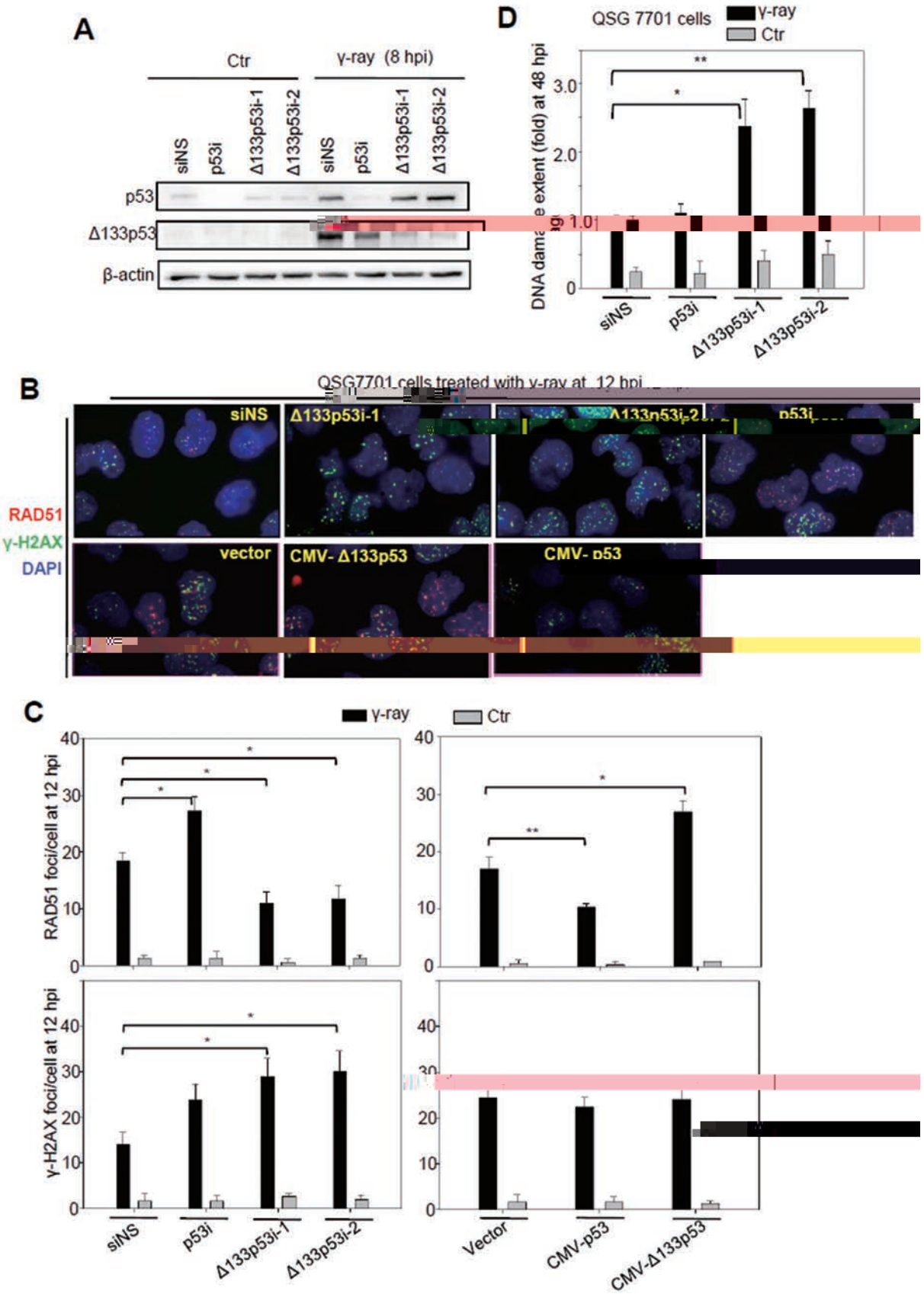
A
Ctr
γ-ray (8 hpi)
siNS
p53i
Δ133p53i-1
Δ133p53i-2
p53
Δ133p53
β-actin
D
QSG 7701 cells
γ-ray
Ctr
DNA damage extent (fold) at 48 hpi
B
QSG7701 cells treated with γ-ray at 12 hpi
RAD51
γ-H2AX
DAPI
vector
CMV- Δ133p53
CMV- p53
C
RAD51 foci/cell at 12 hpi
γ-H2AX foci/cell at 12 hpi
Vector
CMV-p53
CMV-Δ133p53

Figure 4 Δ133p53 promotes RAD51 foci formation and DNA DSB repair in QSG-7701 cells upon ionizing irradiation. **(A)** Western blot analysis of p53 activation and Δ133p53 induction in QSG-7701 cells transfected with non-specifc siRNA (siNS), *p53* interference RNA (p53i) or two Δ*133p53* interference RNAs, Δ133p53i-1 and Δ133p53i-2, followed by 10 gray of γ-ray irradiation. **(B)** Co-immunostaining of RAD51 (in red) and γH2AX (in green) in QSG-7701 cells with different treatments as indicated. The specifc monoclonal antibodies were used to determine the RAD51 and H2AX foci formation at 12 hpi as indicated. DAPI was used to stain the nuclear DNA (blue). **(C)** Statistical analysis of the average number of RAD51 and γH2AX foci per cell in different samples, as shown in **B**. At least 100 cells from each sample were randomly chosen for counting RAD51 and γH2AX foci. **(D)** Assessment of DNA DSB with a comet assay at 48 hpi in QSG-7701 cells with different treatments, as indicated. About 100 cells from each sample were randomly chosen to measure the extent of DNA damage. A statistical analysis was performed based on the data from three repeat experiments.

of 8 out of 14 DNA DSB repair genes (including *lig4 rad54 recq4 wrn rad51 rad52 mre11*) was signifcantly downregulated by p53. Δ113p53 suppressed the inhibitory effect of p53 on the expression of all of these genes except for *wrn* Figure 6B), which may explain Δ133p53's ability to neutralize the inhibitory effect of full-length p53 on DSB repair.

Strikingly, Δ113p53 alone promoted the expression *rad51* (required for HR repair *lig4* NHEJ repair *rad52* (required for SSA repair Figure 6B). We examined the transcriptional activity of human Δ133p53 by transfecting QSG7701 cells with siNS, p53i, 133p53i-1 or Δ133p53i-2 and then treating them with γ-irradiation. The results from both qRT-PCR and protein analyses showed that the expression levels of RAD51, LIG4 and RAD52 were all upregulated at 12 hpi (; Supplementary information, Figure S18). The upregulation of these genes after γ-irradiation was attenuated by knockdown of Δ133p53 and enhanced by knockdown of p53 (; Supplementary information, Figure S18).

We generated two mutants to test whether the function of Δ113p53 in facilitating DNA DSB repair is dependent on its transcriptional activity, ^{R143H} ^{R250W} (the number denotes the mutation's position in the full-length zebrafish *p53* ^{R143H} ^{R250W} correspond to the R175H and R282W mutations in full-length human p53, respectively, which are known to lose their DNA binding capacity . qRT-PCR results showed that, unlike WT Δ113p53, the two Δ113p53 mutants did not upregulate the expression of *rad51 lig4 rad52*). Further experiments demonstrated that the two mutants also failed to promote HR, NHEJ and SSA repairs (Figure 6E

Next, we used zebrafsh $p53^{M214K}$ mutant embryos to investigate the roles of *rad51 lig4 rad52* in the DNA DSB repair pathways, in the context of Δ113p53. Specifc MOs were used to knock down *rad51 lig4 rad52* under different conditions in embryos overexpressing Δ113p53 and an HR, NHEJ or SSA reporter construct. Our results revealed that knockdown of *rad51 lig4 rad52* significantly attenuated the effect of Δ113p53 on promoting DNA DSB repair in the corresponding pathway ( ). All of these data suggested that Δ113p53's transcriptional activity is important for DNA DSB repair.

rad51, lig4 and rad52

A previous study showed that human p53 repressed *RAD51* transcription by directly binding to its promoter . We tested whether Δ113p53 also has a direct role in *rad51* transcription by cloning the zebrafsh *rad51* moter of 5 kb upstream of the *rad51* transcriptional start site and generating the *rad51p:Egfp* reporter construct Figure 7A). This 5-kb fragment recapitulates the pattern *rad51* expression in response to p53 and Δ113p53 expression (Figure 7B). Two putative p53 REs were found within the promoter region of *rad51* at positions –3 384 and –1 165 nucleotide (Figure 7A). Interestingly, the arrangements of four pentamers found in both of the REs are novel compared to those reported previously (Figure 7A). We found that the deletion of RE1 switched the effect of p53 from repressing to promoting *Egfp* expression. The deletion of RE2 abrogated the effect of Δ113p53 but enhanced the suppressing effect of Figure 7B). A gel retardation experiment revealed that both p53 and Δ113p53 could bind to RE2, whereas only p53 could bind to RE1 ( ). These results suggest that p53 first binds to RE1 to suppress *rad51* expression. In the absence of RE1, p53 binds to RE2 to promote *rad51* expression, and RE2 serves as the sole site for Δ113p53 binding to promote *rad51* expression.

Further analysis showed that the p53-repressing RE (RE1) and Δ113p53-activating RE (RE2) were also present in zebrafish *rad52 lig4* promoters (*RAD51 LIG4 RAD52* promoters (Supplementary information, Figure S19). A chromatin immunoprecipitation (ChIP) assay was performed to study whether p53 and Δ113p53 bind to their respective REs in the promoters of three DNA DSB repair genes *in vivo* upon γ-irradiation. As shown in Figure 1B, expression

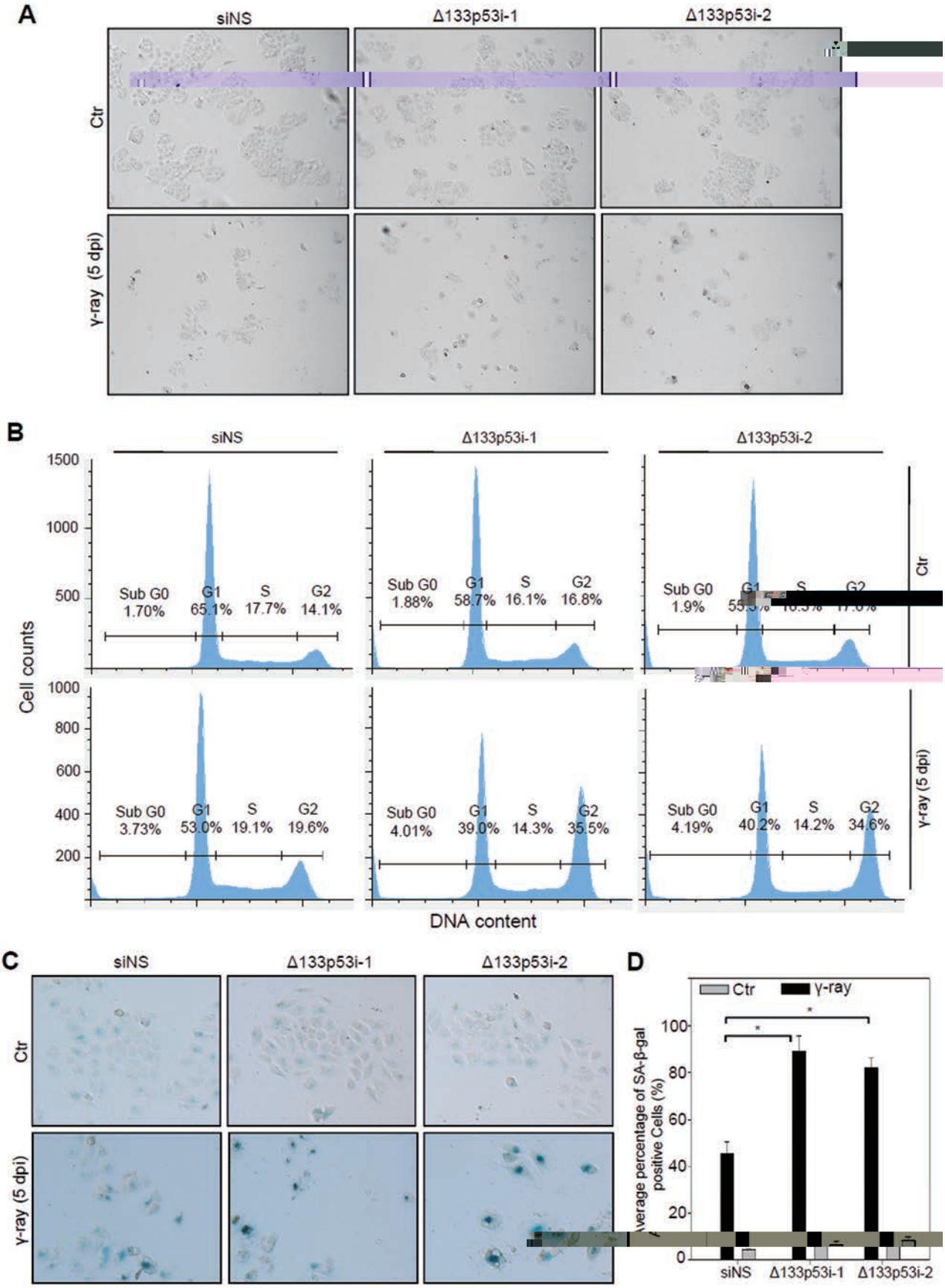
A
siNS
Δ133p53i-1
Δ133p53i-2
Ctr
γ-ray (5 dpi)
B
siNS
Δ133p53i-1
Δ133p53i-2
Cell counts
Sub G0 1.70%
G1 65.1%
S 17.7%
G2 14.1%
Sub G0 1.88%
G1 58.7%
S 16.1%
G2 16.8%
Sub G0 1.9%
Ctr
Sub G0 3.73%
G1 53.0%
S 19.1%
G2 19.6%
Sub G0 4.01%
G1 39.0%
S 14.3%
G2 35.5%
Sub G0 4.19%
G1 40.2%
S 14.2%
G2 34.6%
γ-ray (5 dpi)
DNA content
C
siNS
Δ133p53i-1
Δ133p53i-2
Ctr
γ-ray (5 dpi)
D
Ctr
γ-ray
Average percentage of SA-β-gal positive Cells (%)
siNS
Δ133p53i-1
Δ133p53i-2

Figure 5 Knockdown of Δ133p53 arrests cell growth at the G2 phase and promotes cell senescence upon γ-irradiation. **(A)** Cell colony formation of irradiated cells. QSG-7701 cells transfected with non-specifc siNS, Δ133p53i-1, or Δ133p53i-2 siRNA were treated with 10 gray of γ-ray irradiation. The pictures were taken at 5 dpi. **(B)** FACS analysis of the percentage of cells at different cell cycle phases based on Propidium Iodide (PI) staining. QSG-7701 cells transfected with siNS, Δ133p53i-1, or Δ133p53i-2 siRNA at 5 dpi as indicated. **(C)** SA-β-gal staining to analyze the senescence status in the QSG-7701 cells with different treatments as described in **B**. **(D)** Statistical analysis of the senescent cells in different samples shown in **C**.

of full-length p53 reached its peak level at 4 hpi, while Δ113p53 expression peaked at 24 hpi. Based on this, we used untreated embryos as the controls and sampled irradiated embryos at 4 and 24 hpi. We used the A7-C10 zebrafish p53 monoclonal antibody, recognizing both p53 and Δ113p53, to perform ChIP experiment. First, we validated our ChIP products by analyzing the occupancy of p53 on the two known p53 REs in the promoter by qPCR. The enrichment of both p53 RE1 and RE3 of the Δ113p53 promoter in the ChIP products was nicely correlated with the dynamic expression levels of p53 at 4 and 24 hpi (Supplementary information, Figure S18A). Next, we examined the occupancy of p53 and Δ113p53 in the promoters of *rad51* *rad52* *lig4* The qPCR analysis showed that RE1 sequences (p53-repressing RE) of *rad51* *rad52* *lig4* were all enriched in the ChIP products from the 4-hpi samples (Figure 7E As the expression level of p53 peaked at 4 hpi (1B), this result suggests that occupancy of RE1 in these promoters by p53 at this stage locks the expression of these genes at a repressive status. In contrast, RE2 sequences (Δ113p53-activating RE) of *rad51* *rad52* *lig4* were all enriched in the ChIP products from the 24-hpi samples (Figure 7E). As the level of Δ113p53 greatly exceeds that of p53 at 24 hpi (Figure 1B), these results demonstrate that the promoters of the three genes are switched from a status of repression by p53 at RE1 to a status of activation by Δ113p53 at RE2 *in vivo*. This occurs as a consequence of the dynamic change of expression levels of p53 and Δ113p53, from 4 to 24 hpi.

To analyze whether the binding of Δ113p53 to RE2 of these three DNA DSB repair gene promoters is independent of full-length p53, we overexpressed HA-p53 and HA-Δ113p53 in *p53* mutants. An HA monoclonal antibody was used to perform the ChIP assay. The assay demonstrated that RE1 was enriched in the ChIP products from the sample overexpressing HA-p53, whereas the sample overexpressing HA-Δ113p53 showed enrichment at RE2 in the promoters of zebrafish *lig4* *rad52* *rad51* (Supplementary information, Figure S20), further confrming the ChIP assay results performed with irradiated zebrafsh embryos. These results demonstrate that Δ113p53 upregulates the expression of *rad51* *lig4* *rad52* by binding to a novel type of p53 REs in their promoters.

Discussion

Up to 13 human p53 isoforms have been identified, and these isoforms are generated through alternative initiation of translation, use of an internal promoter or alternative splicing . p53 isoforms can modulate p53 functions either synergistically or antagonistically, depending on the isoform's structure and the target genes affected . However, how these isoforms affect DNA damage repair is rarely studied. Many studies have demonstrated that full-length p53 inhibits DNA DSB re . A recent study using human cells has shown that, in response to γ-irradiation treatment, p53 pulses induce apoptosis at the early stage and postpone DNA DSB repair to the later stage . Here, we found that the p53 isoform Δ113p53/Δ133p53 is strongly induced by γ-irradiation, but not by UV irradiation and heat shock treatment. Interestingly, we observed that, upon γ-irradiation, the levels of full-length p53 and Δ113p53p53 proteins in the treated zebrafsh embryos were differentially expressed. Full-length p53 protein level peaked early, at 4 hpi, whereas Δ113p53p53 protein level peaked later, at 24 hpi. We showed previously that Δ113p53/Δ133p53 is a p53 target gene and inhibits p53-mediated apoptosis by modulating the expression of p53 target genes . All of our fndings imply that Δ113p53/Δ133p53 may coordinate with full-length p53 to regulate cell death and DNA DSB repair in response to DNA DSB stress. Through Egfp-repairing-aided visual-plus-quantitative analysis reporter systems, comet assay and repair foci analysis, we demonstrated that Δ113p53/Δ133p53 promotes all three DNA DSB repair pathways in both zebrafsh and human cells in a p53-independent manner. Further experiments with γ-irradiated zebrafish embryos showed that the proportion of apoptotic cells peaked around 8 hpi and dropped to the basal level at 24 hpi, which correlated well with the level of full-length p53 protein. In contrast, the extent of DNA damage decreased rapidly after 28 hpi, corresponding to the level of Δ113p53 protein. We revealed how changes in the levels of p53 and Δ113p53 proteins regulate cell death and DNA DSB repair in response to DNA damage. To minimize DNA DSBs as the frst defense at the early stage of DNA damage response, full-length p53 is induced to a high level to guide cells

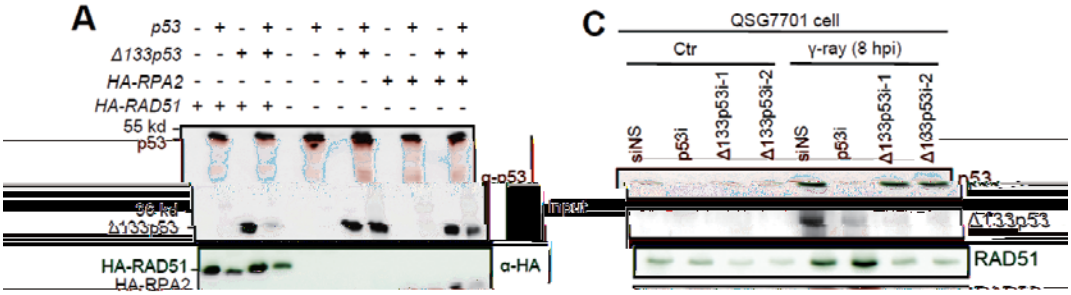
A
p53
Δ133p53
HA-RPA2
HA-RAD51
55 kd
p53
α-p53
IP:HA
HA-RAD51
α-HA
C
QSG7701 cell
Ctr
γ-ray (8 hpi)
siNS
p53i
Δ133p53i-1
Δ133p53i-2
RAD51

Figure 6 Δ113p53/Δ133p53 promotes DNA DSB repair by upregulating the expression of *Rad51*, *Rad52* and *Lig4*. **(A)** Co-IP analysis of the interaction between p53 or Δ133p53 with HA-RAD51 or HA-RPA2 in H1299 cells. An anti-HA antibody was used in an immunoprecipitation. Proteins from co-IP were detected with a p53 CM1 antibody (third panel) and the HA antibody (fourth panel). The 10% of input from each sample was used as a control: top panel p53 (CM1); second panel: HA. **(B)** Relative mRNA expression of the listed genes in zebrafsh $p53^{M214K}$ mutant embryos overexpressing Δ*113p53*, *p53* or both *p53* and Δ*113p53* measured by qRT-PCR at 8 hpf. Gene expression was normalized against 18S rRNA and expressed as the fold change compared to the injection control. **(C)** Western blot analysis of proteins in human QSG7701 cells with different treatments as indicated. **(D)** Relative mRNA expression of the listed genes in zebrafsh $p53^{M214K}$ mutant embryos overexpressing Δ*113p53*, $\Delta 113p53^{R143H}$ or $\Delta 113p53^{R250W}$ measured by qRT-PCR. **(E)** Effects of Δ*113p53*, $\Delta 113p53^{R143H}$ and $\Delta 113p53^{R250W}$ on HR, NHEJ and SSA repair frequencies. The average repair frequencies were measured by qPCR analysis of different repaired assay constructs from three repeat experiments at 10 hpf. **(F)** The activity of *rad51*, *lig4* and *rad52* was required for zebrafsh Δ113p53-meadited HR, NHEJ and SSA repairs. The rad51-MO, lig4-MO or rad52-MO was used to knock down its corresponding gene expression in the HR, NHEJ or SSA analysis. The average repair frequencies were measured with a qPCR analysis of the repaired assay constructs from three repeat experiments at 10 hpf. Different lanes are numbered; v: versus, *t*-test between two lanes.

with severe DNA damage to undergo apoptosis. The subsequent expression of Δ113p53, as the second wave of defense, inhibits apoptosis in the remaining cells with repairable DNA damage and, at the same time, promotes DNA DSB repair. Our fndings demonstrate that Δ113p53/Δ133p53 is a pro-survival factor and may also imply possible roles of the other p53 isoforms in different DNA damage repair pathways.

The importance of Δ113p53/Δ133p53 for cell survival and its signifcance to the survival of a whole organism is further demonstrated in the $^{M/M}$ mutant. Although the $^{M/M}$ mutant zebrafsh grows normally in standard growth conditions, it is sensitive to γ-irradiation. No mutant embryos were able to survive longer than 5 days after irradiation, while irradiated WT embryos exhibited a survival rate of about 30%. Sensitization to γ-irradiation is due to an increase in both apoptotic activity and the extent of DNA damage in the $^{M/M}$ mutant embryos upon irradiation. The fact that the mortality of irradiated $^{M/M}$ mutant embryos was much higher than that of irradiated WT embryos, even when apoptosis was inhibited by *bcl2* mRNA injection, strongly suggests that in addition to its anti-apoptosis activity, the function of promoting DSB damage repair of Δ113p53 is crucial in protecting an organism from DNA damage. Similarly, in human cells the ratios of cells at the G2 phase and SA-β-gal-positive cells were signifcantly higher in irradiated Δ133p53-knockdown cells, which eventually resulted in smaller colony sizes and fewer colonies. A previous study reported that the basal expression of Δ133p53 inhibits p53-mediated replicative senescence through downregulating the expression of $p21^{WAF1}$ *miR-34a* in normal human fibroblasts . Δ133p53 knockdown-induced senescence was accompanied by the attenuation of BrdU (bromo-deoxyuridine) incorporation, which suggests that the cell senescence was due to cell cycle arrest at the G1 . In this study, we showed that knockdown of Δ133p53 in cells exposed to DNA DSB stress also resulted in cell senescence. However, this senescence was caused by unrepaired DNA DSBs and accompanied by the increase of cells at the G2 phase. These results suggest that Δ133p53 regulates cell replicative senescence in the normal condition and cell senescence upon a DNA damage stress by different mechanisms.

One important rationale for p53 inhibition of DNA DSB repair is its direct interactions with repair proteins, such as RAD51 and RPA, to prevent repair complex formation. The key residues in human p53's DNA binding core domain (including residues 102, 103, 105, 114, 115, 122 and 126) are required for interactions with RAD51, and those in the N-terminal motif (residues 37-57) are required for interactions with RPA. These key amino acid residues are absent in the Δ133p53 protein
might be the reason that Δ133p53 was not co-immunoprecipitated with RAD51 and RPA in this study. However, Δ133p53 may interrupt the interaction between p53 and HA-Rad51 or HA-RPA2, which was probably due to Δ133p53's ability to form a hetero-complex with p53 , which may allow it to neutralize the DSB repair inhibitory effect of full-length p53.

Δ113p53/Δ133p53 is an N-terminally truncated protein without the transactivation domain. Our previous studies showed that, although co-expression of Δ113p53 and p53 alters the expression patterns of p53 downstream genes such as *p21 mdm2 bcl2L*, expressing Δ113p53 alone results in little transcriptional activity on these genes in the $p53^{M214K}$ mutant background . Surprisingly, here we found that Δ113p53 upregulates the expression of the DNA DSB repair genes *rad51 lig4 rad52*
dent of full-length p53. The transcriptional activity of Δ113p53 is required for its positive effect on DNA DSB repair as, apart from impairing its transcriptional activity, mutations in its DNA-binding domain also abolished its ability to promote DNA DSB repair. Through promoter

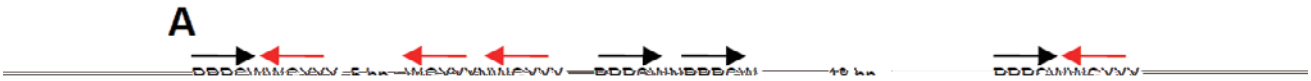
A

Figure 7 Δ113p53 upregulates the expression of *rad51*, *rad52* and *lig4* by directly binding to a new type of p53 RE in their promoter regions. **(A)** The *rad51* promoter. The black and red arrows correspond to the orientations of the quarter sites. R = A or G, W = A or T, Y = C or T. The positions of two p53 REs in the *rad51* promoter are indicated. **(B)** Northern blot analysis of the transcription levels of endogenous *rad51* and *Egfp* in *p53*^{M214K} mutant embryos injected with *rad51p:Egfp*, *rad51p-ΔRE1:Egfp* (with a 26-bp deletion of RE1), *rad51p-ΔRE2:Egfp* (with a 39-bp deletion of RE2) and *rad51p-ΔRE1+2:Egfp* (with double deletions in RE1 and RE2) plasmids, or co-injected with these plasmids and *p53*, Δ*113p53* or *p53*-plus-Δ*113p53* mRNAs, as indicated. 28S rRNA was used as the loading control. The numbers between the panels are the relative gene expression levels normalized against 28S rRNA in each experiment. **(C)** EMSA was performed to detect p53 and Δ113p53 interactions with RE1 and RE2 in the *rad51* promoter. The 26-bp DNA fragments of RE1 and an RE1 mutant with 6 bp mutated (AGAAATACAC AATAA TTTTCATTTAT; mutations are underlined), and 39-bp DNA fragments of RE2 and an RE2 mutant with 6 bp mutated (ATATAAAAATA GAATCCCAAAAATTAAGT GAAAAATTAT; mutations are underlined) of the *rad51* promoter were labeled with biotin to form probes. Nuclear proteins were extracted from zebrafish *p53*^{M214K} mutant embryos injected with different mRNAs as indicated. Labeled probes were incubated with different protein extracts, with unlabeled probes and zebrafish A7-C10 antibody, as indicated. **(D)** *p53* and Δ*113p53* REs in *rad52* and *lig4* promoters compared to other *p53* REs. Mismatch nucleotides are labeled red. The positions of p53 REs in the respective promoters are indicated. **(E)** ChIP of RE1 and RE2 in *rad51*, *rad52* and *lig4* promoters in the irradiated embryos at 4 and 24 hpi. WT embryos were treated with γ-irradiation and sampled at 4 and 24 hpi, respectively. The A7-C10 p53 antibody was used to co-immunoprecipitate the protein-DNA complex, while IgG was used as a non-specific binding control. Specific primer pairs were designed to amplify the corresponding REs. DNA was normalized with a pair of negative control primers for β-actin exon. The results are presented as the relative occupancies of different REs. Statistics were obtained from three repeat experiments.

functional analysis, gel shift and ChIP assays, we demonstrated that Δ113p53 binds to a novel type of p53 RE in the promoters of zebrafish *rad51* *lig4* *rad52*. A similar type of RE was also found in the promoter re *RAD51* *LIG4* *RAD52*. It is currently unclear how Δ113p53/Δ133p53 lacking the transactivation domain of full-length p53 exerts a transcriptional activity independent of full-length p53. A recent study showed that p53 isoforms, including Δ133p53, differentially regulate p73 transcriptional activities by protein interactions , which suggests that Δ113p53/Δ133p53 may interact with p73 or its isoforms to achieve its transcriptional activity.

From an evolutionary point of view, given a DNA damage stress condition, the first, crucial action taken by an organism is to survive under such environment. The second action is to minimize genetic insults to avoid genetic diseases during the course of development and reproduction. Here, we demonstrate that the Δ113p53/Δ133p53 is a pro-survival factor for DNA damage stress, and induction of its expression prevents apoptosis and promotes DNA DSB repair, thus inhibiting cell senescence. However, whether Δ113p53/Δ133p53 also plays a role in preventing diseases in response to DNA damage needs to be further explored. It would be very interesting to know whether the $^{M/M}$ mutant exhibits a shortened life-span and high frequency of tumorigenesis in response to low dosage of γ-irradiation.

About 60% of all cancer patients are treated with radio-therapy alone or in combination with other anticancer treatments, including surgery . Most patients can tolerate radiation treatment well, with 5%-10% suffering severe side effects in normal tissue. This radio-sensitivity is partly genetically determined. A few molecular markers have been successfully applied to predict the radio-sensitivity in individual patients Here, we demonstrate that Δ133p53 is strongly induced by ionizing radiation and protects cells from death and senescence through preventing apoptosis and promoting DNA DSB repair, which suggests that the induction of expression in normal cells and tissues provides a potential marker to assess a patient's tolerance to radiation treatment.

Materials and Methods

Zebrafish was raised and maintained in standard zebrafish units at Zhejiang University. The *p53* mutant allele *p53*^{M214K} line was provided by professor Thomas Look at Harvard Medical School (Boston, USA).

Cell culture

H1299 (TCHu160) and QSG-7701 (GNHu7) cells were purchased from the cell bank of the Chinese Academy of Sciences (Shanghai, China). HR-U2OS was a gift from professor Huang Jun at Zhejiang University (Hangzhou, China). Plasmids and siRNAs were transfected into cells with FuGENE HD (Roche) and Lipofectamine 2000 transfection reagents, respectively.

HR, NHEJ and SSA assays

The construction of the HR, SSA and NHEJ visual-plus-quantitative assay systems and analyzing procedures were performed as described previously (Supplementary information, Figure S2). The primers used in qPCR are listed in Supplementary information, Table S1.

The H1299 cell line was used for HR, SSA, and NHEJ assays in human cells. 1.5 μg of I-SceI-cut HR, 0.5 μg of I-SceI-cut

NHEJ or 0.5 μg of I-SceI-cut SSA plasmid DNA was co-transfected with 0.5 μg of CMV-p53, 1.5 μg of CMV-Δ133p53 or 0.5 μg of CMV-p53 with 1.5 μg of CMV-Δ133p53 into 1 × H1299 cells. An uncut plasmid was transfected as the negative control. Transfected cells were cultivated for 24 h at 37 °C and subsequently subjected to FACS analysis with a FACS Calibur Flow Cytometer (BD Biosciences). A minimum of 10 000 cells per sample were analyzed. DNA was also extracted at 24 hpt for qPCR analysis, as described above.

Zebrafish embryos at 24 hpf were irradiated with a dose of 16 gray of γ-ray from a Cs source. For UV-irradiation treatment, embryos at 24 hpf were treated with a total energy of 75 mJ/cm UV irradiation by a UV source (UV-CL-1000 Ultraviolet Crosslinker) emitting 254 nm light (UVP, USA). For heat shock treatment, 24-hpf embryos, growing at 28.5 °C, were transferred to a °C growth chamber until protein extraction.

For γ-irradiation in human cell lines, untreated or transfected cells at 24 hpt were irradiated with a dose of 10 gray of γ-ray. For UV-irradiation treatment, cells were treated with a total energy of 30 mJ/cm UV. For heat shock treatment, cells cultured at 37 ° were transferred to a 42 °C growth chamber for 8 h and then returned to 37 °C until protein extraction.

Comet assay

For the comet assay in zebrafish, ~100 irradiated or un-irradiated control embryos were sampled at 28 and 36 hpi, and subjected to cell dissociation in ice-cold PBS containing 20 mM EDTA (without Mg). The comet assay was performed with a OxiSelectTM comet assay kit (3-well slides, Cell Biolabs Inc.) according to the manufacturer's recommendations. Embedded cells were treated with a lysis buffer at pH 7 without alkaline treatment to release the double-stranded DNA. For data processing, each comet picture was measured with the software ImageJ 1.45 (National Institutes of Health) and the extent of damage in individual cells was calculated as described in Supplementary information, Figure S6.

For the comet assay in the human cell line, QSG7701 cells were transfected with siRNAs, followed by γ-irradiation, as described in the apoptosis and cell cycle assay. The irradiated cells were fixed in 70% ethanol at 48 hpi and subjected to the comet assay, as described in the zebrafish comet assay.

Zebrafish *p53* *bcl2L* were constructed as described previously was amplified using the primer pair *HA HuRad51 BamHI* *HA HuRad51 XbaI*-Rev. Human *HA-RPA2* was amplified using the primer pair *HA HuRPA2 BamHI* *HA HuRPA2*-Rev-*EcoRI*. The primer sequences are provided in Supplementary information, Table S1.

$^{M/M}$ mutant with the TALEN technique

promoter is located in the fourth intron of the full-length *p53* . The third p53 RE in the promoter (5′-cagtggaggttGAACATGTCTGAACTTGTCCtgattgagcagtggggg-3′; the sequence of p53 RE is shown in upper case) was chosen for the TALEN targeting site . We placed the third p53 RE at the spacer region where indels often occur. The two TALEN plasmids with the target binding sites (shown in red letters in Figure 2A) were ordered from ViewSolid Biotech. The two TALEN mRNAs were prepared and co-injected into WT embryos at one-cell stage according to the manufacturer's recommendations.

The TALEN-injected embryos were raised to adulthood and outcrossed with WT fish. The F1 embryos were used to identify mutant founders. The tail of F1 adult fish was used to identify heterozygous mutants. To identify the genetic mutants, a pair ′-GGCAGTCTAGCTTATGTGT-3′ ′ GACTGTCCAGCACTA-3′) flanking the target site, were used to amplify a 400-bp DNA fragment from genomic DNA. The PCR product contains a digestion site of the restriction enzyme *Hpy*188III around the third p53 RE. The PCR fragment from WT can be digested into two 200-bp bands, while the PCR fragment from a mutant remains as a 400-bp band. The fragment deletions were subsequently confirmed by sequencing.

For SA-β-gal staining, QSG7701 cells were transfected with siRNAs followed by γ-irradiation, as described in the apoptosis and cell cycle assays. At 48 hpi, the irradiated cells were fixed in 4% PFA and subjected to SA-β-gal staining with Cell Senescence SA-β-Gal Staining Kit (Beyotime, C0602). Statistics was obtained from three repeat experiments.

rad51 promoter reporter assay

A 5.0-kb DNA fragment upstream of the transcriptional start site of *rad51* Figure 7A) was amplified from genomic DNA (AB strain WT zebrafish) with the primer pair *rad51* *XhoI* *rad51* *BamHI*-Rev, and cloned into the pEgfp-1 vector to generate the plasmid *rad51p:Egfp*. The single motif deletion promot *rad51p RE1:Egfp* *rad51p-RE2:Egfp* Figure 7B) were amplified from the *rad51p:Egfp* plasmid using their respective primer pairs. The primers sequences used are listed in Supplementary information, Table S1. The promoter with a double-deletion, was generated from the single deletion plasmid.

RNA analysis

For northern blot hybridization, full-length *Egfp* bp DNA fragment of *rad51* cDNA were labeled with Digoxigenin (DIG) to form probes. qRT-PCR in zebrafish was performed as described previously . The primer sequences and accession numbers of the analyzed genes are listed in Supplementary information, Table S1.

Electrophoretic mobility shift assay (EMSA)

Twenty-six-bp DNA fragments of RE1 and an RE1 mutant with 6 bp mutated, and 39 bp of RE2 and an RE2 mutant with 6 bp mutated of the *rad51* promoter ( ) were artificially synthesized and labeled with biotin as probes (Shanghai Sangon). Nuclear proteins were extracted from injected embryos at 8 hpf with a nuclear protein and cytoplasm protein extraction kit (Beyotime, P0027). Forty fmol of labeled probe was incubated with 2 μg of extracted nuclear protein for 20 min. To specifically block band shift, 8 pmol of unlabeled probe or 200 ng of A7-C10 zebrafish p53 monoclonal antibody was added to the mixture and incubated for 20 min. Labeled biotin was analyzed with a light shift chemiluminescent EMSA kit (Pierce, 20148), according to the manufac

turer's instructions.

ChIP assay

ChIP assays were performed as described previously For immunoprecipitation of endogenous p53 and Δ113p53, WT embryos were treated with 16 gray of γ-ray. Untreated embryos, and irradiated embryos at 4 and 24 hpi were sampled. Chroma tin was sheared into 200-800-bp fragments with Cole-Parmer sonicator equipped with a 2-mm tip. The A7-C10 zebrafsh p53 antibody was used to perform immunoprecipitation with the soni cated DNA-protein complex solutions, while IgG was used as the non-specifc binding control with the same amount of the sonicat ed solution. Primers used in qPCR are listed in Supplementary in formation, Table S1. Total pulled down DNA was normalized with a pair of non-specifc primers for the β-actin exon. The specifc primers for p53 RE1 and RE3 of the promoter were used as a p53-binding positive control

To immunoprecipitate ectopically expressed HA-p53 and HA-Δ113p53, ~40 pg of pGEMT plasmid was injected alone, or co-in jected with 50 pg of *HA p53* mRNA and 300 pg of *HA* mRNA, into one-cell-stage embryos. At 7 hpf, injected embryos from each treatment were sampled. HA antibody matrix (Abmart) was used for immunoprecipitation. Total DNA was normalized with exon-specific primers. Meanwhile, p53, RE1, and RE3 of promoter were used as p53-binding positive control.

Western blotting was performed as described previously Zebrafish p53 monoclonal antibody (A7-C10) was generated as described

For co-IP analysis, transfected cells were cultivated for 24 h at 37 °C, followed by protein extrac t ! ₤ ᴰ φ ɾ ! eatrix mAbmart)

ieaeafrr ^ rbr § r - eeb £ eecex £ ^ rm l ą Ů cde £ m Ἃ ꝺ ș ɰ ᴰ ä cbr § cd ´ hx@ccee cbex £ - e - ¤ l- cb}e - ¤ - e

recombination. *Cancer Res* **63**

17 Boehden GS, Akyuz N, Roemer K, Wiesmuller L. p53 mutat ed in the transactivation domain retains regulatory functions in homology-directed double-strand break repair. *Oncogene*

18 Buchhop S, Gibson MK, Wang XW, *et al*. Interaction of p53 with the human Rad51 protein. *Nucleic Acids Res*

19 Romanova LY, Willers H, Blagosklonny MV, Powell SN. The interaction of p53 with replication protein A mediates suppression of homologous recombination. *Oncogene*

20 Arias-Lopez C, Lazaro-Trueba I, Kerr P, *et al.* p53 modulates homologous recombination by transcriptional regulation of the *RAD51* *EMBO Rep*

21 Purvis JE, Karhohs KW, Mock C, *et al.* p53 dynamics control cell fate. *Science* **336**

22 Zhang XP, Liu F, Cheng Z, Wang W. Cell fate decision medi ated by p53 pulses. *Proc Natl Acad Sci USA*

23 Bourdon JC, Fernandes K, Murray-Zmijewski F, *et al.* isoforms can regulate p53 transcriptional activity. *Genes Dev*

24 Chen J, Ruan H, Ng SM, *et al.* Loss of function of def selec tively upregulates {Delta}113p53 expression to arrest expan sion growth of digestive organs in zebra f sh. *Genes Dev*

25 Chen J, Peng J. p53 isoform delta113p53 in zebra f sh. *Zebraf- ish* **6**

26 Chen J, Ng SM, Chang C, *et al.* p53 isoform delta113p53 is a p53 target gene that antagonizes p53 apoptotic activity via BclxL activation in zebra f sh. *Genes Dev*

27 Marcel V, Vijayakumar V, Fernandez-Cuesta L, *et al.* regulates the transcription of its Delta133p53 isoform through speci f c response elements contained within the TP53 P2 in ternal promoter. *Oncogene*

28 Aoubala M, Murray-Zmijewski F, Khoury MP, *et al.* directly transactivates Delta133p53alpha, regulating cell fate outcome in response to DNA damage. *Cell Death Differ*

29 Fujita K, Mondal AM, Horikawa I, *et al.* p53 isoforms Del ta133p53 and p53beta are endogenous regulators of replica tive cellular senescence. *Nat Cell Biol*

30 Bernard H, Garmy-Susini B, Ainaoui N, *et al.* form, delta133p53alpha, stimulates angiogenesis and tumour *Oncogene*

et al. Development of novel visu al-plus quantitative analysis systems for studying DNA dou ble-strand break repairs in ή ! b